Inorganica Chimica Acta 502 (2020) 119372

Contents lists available at ScienceDirect

Inorganica Chimica Acta

journal homepage: www.elsevier.com/locate/ica

Research paper

A dual colorimetric chemosensor based on Schiff base for highly selective and simultaneous recognition of CN^- and Sn^{2+}

Pravin R. Dongare[a], Anil H. Gore[b], Balu D. Ajalkar[a,*]

[a] Department of Chemistry, Shivraj College of Arts, Commerce and D. S. Kadam Science College, Gadhinglaj, Affiliated to Shivaji University, Kolhapur, Maharashtra 416 502, India

[b] Department of Chemistry, Uka Tarsadia University, Bardoli- Mahuva Road, Tarsadi, Gujarat 394 350, India

ARTICLE INFO

Keywords:
Schiff base
Azo dye
Dual colorimetric chemosensor
Cyanide ion
DFT

ABSTRACT

A new colorimetric chemosensor 2-methoxy-6-{(*E*)-[(4-methylphenyl)imino] methyl}-4-[(*E*)-(4-nitrophenyl) diazenyl] phenol (**SZ**) was designed and synthesized for simultaneous detection of CN^- and Sn^{2+} in MeCN: bis-tris buffer solution. The sensor **SZ** showed quick and selective colorimetric response towards CN^- and Sn^{2+} with a change in color from yellow to pink and colorless respectively without any interfering anions or cations. Meanwhile, the binding mode of **SZ** for CN^- and Sn^{2+} were studied by ^1H NMR, ESI-MS, FT-IR spectroscopy, Job's plot analysis and DFT calculations. The detection limit of **SZ** towards CN^- and Sn^{2+} was found to be 0.649 μmol/L and 0.754 μmol/L respectively which are lower than the WHO guidelines for drinking water. Furthermore, chemosensor **SZ** was successfully utilized as a colorimetric chemosensor for the detection of CN^- and Sn^{2+}.

1. Introduction

The design of colorimetric chemosensor for selective sensing of biologically and chemically important anions and cations has received huge interest in the past decade [1–6]. Among these cyanide gives particular interest for their toxicity to environment and life system because, cyanide is readily absorbed through alimentary canal, lungs, skin and has strongest binding affinity to ferric ion present in the enzyme cytochrome-c oxidase, which inhibit the mitochondrial electron transport chain results loss of consciousness, convulsion, palpitation and death [7–9]. Nevertheless, cyanide is widely used in industrial processes, such as textile manufacturing, metallurgy, silver production, herbicides and gold mining which has led to the inadvertent release of cyanide from industrial waste which is harmful to environmental and aquatic life [10–13].

Besides, tin is a soft, silvery-white post-transition metal commonly used in dentifrices, catalysts in the preparation of indole and coumarin derivatives, biodiesel [14–17]. Further, tin is an essential trace mineral for humans and is found in the thyroid gland, liver, spleen and brain [18,19]. It also involved in the hair growth and prevention of cancer in human beings [20,21]. The deficiency of tin results in decreased hearing loss, shortness of breath, asthma and diminished hemoglobin synthesis. While, excess accumulation of tin finds some severe immunotoxic and neurotoxic effects in human cause symptoms generally gastrointestinal complaints such as nausea, diarrhea, vomiting and cramps [22,23].Therefore, it is important to develop chemosensor for the determination of CN^- and Sn^{2+} in an aqueous medium.

In earlier several modern analytical methods for detection of CN^- and Sn^{2+} ion has been developed such as ion-exchange chromatography [24], electrochemical methods [25,26], flow injection [27] and atomic absorption spectroscopy [28] required sophisticated equipment, trained operators and are time-consuming. But, colorimetric chemosensors for the detection of different ions pay special attention of the researchers of chemical, environmental sciences owing to their wide range of advantages such as high selectivity, sensitivity, low cost and direct visual detection of color change without the use of any expensive instruments [29,30]. Therefore, it is necessary to develop a colorimetric sensor that is capable of recognizing both CN^- and Sn^{2+}.

Schiff bases are the product of condensation reaction between the aromatic amine and aromatic aldehyde or ketone commonly acts as an important class ligand in various metal complexes. Moreover, due to their easy synthesis, solubility in common solvents, structural modification, selectivity towards specific metal ion in presence of other ions due to the unique size of the ion, charge on the metal ion and the hard-soft acid-base nature of metal and donor atom from the Schiff base, they have been successfully used as highly selective and sensitive sensing material for detection of ions in several optical, electrochemical or membrane chemosensors [31,32]. Further, Schiff bases containing

* Corresponding author.
E-mail address: bajalkar@rediffmail.com (B.D. Ajalkar).

https://doi.org/10.1016/j.ica.2019.119372
Received 3 November 2019; Received in revised form 14 December 2019; Accepted 14 December 2019
Available online 17 December 2019

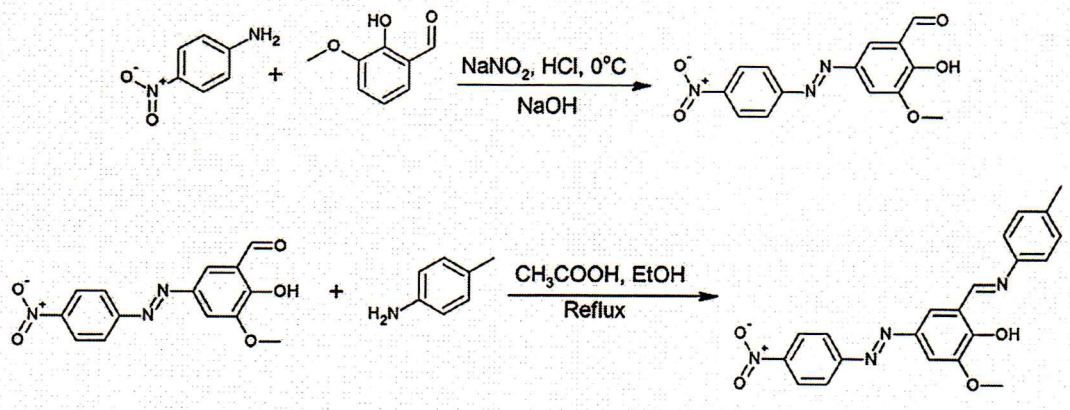

Scheme 1. Synthesis of Chemosensor **SZ**.

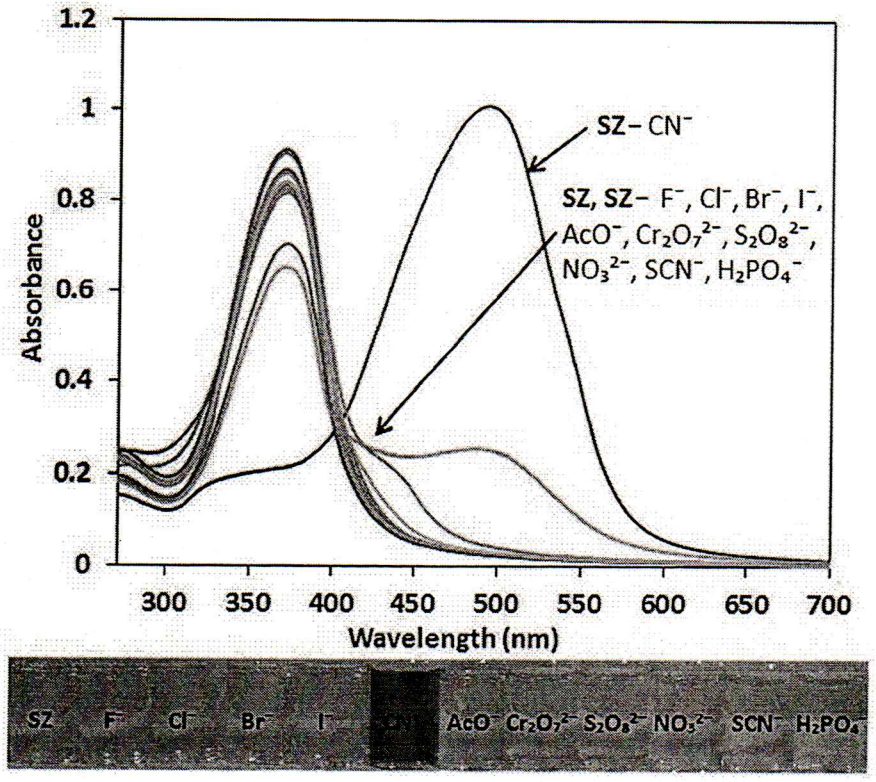

Fig. 1. UV–Vis absorbance spectra of **SZ** (30 μmol/L) in presence of different anions (150 μmol/L) in MeCN: bis-tris buffer (9:1, v/v; pH = 7.0) solution.

salicyaldimine based ligands in conjugation with azo chromophore can be used in the development of inexpensive colorimetric chemosensors as they show rapid response rate, excellent color changes of the solution and strong ability to form charge transfer complexes when they interact with cations and anions [33].

In view of this herein we developed a colorimetric chemosensor **SZ** based on azo chromophore containing Schiff-base for selective and simultaneous detection of CN^- and Sn^{2+} in an aqueous organic medium in which CN^- is sensed by deprotonation of a phenolic hydroxyl group and Sn^{2+} by azomethine group in Schiff base which acts as ligand towards Sn^{2+}. The sensor **SZ** detect CN^- and Sn^{2+} by a change in color from yellow to pink and yellow to colorless respectively with high selectivity via naked eye in CH_3CN/H_2O (9:1, v/v) solution among other tested ions. The interaction of **SZ** with CN^- and Sn^{2+} was investigated using UV–Vis absorption, FT-IR, ^1H NMR, ESI-mass spectral techniques and theoretically supported by Density Functional Theory (DFT) calculations.

2. Experimental

2.1. Materials and measurements

p-Nitroaniline, vanillin and *p*-toluidine were purchased from Sigma-Aldrich and used without further purification. Salts of different cations and anion were purchased from S. D. Fine-Chem. Ltd. (Mumbai, India). All the analytical grade (A. R.) solvents ethyl alcohol, acetonitrile were purchased from Research-lab fine Chem, Mumbai and Spectrochem, Mumbai, India respectively and used without further purification. The ^1H NMR and ^{13}C NMR spectra were recorded on a Bruker AC 300 MHz NMR spectrometer using DMSO-d_6 as solvent and tetramethylsilane

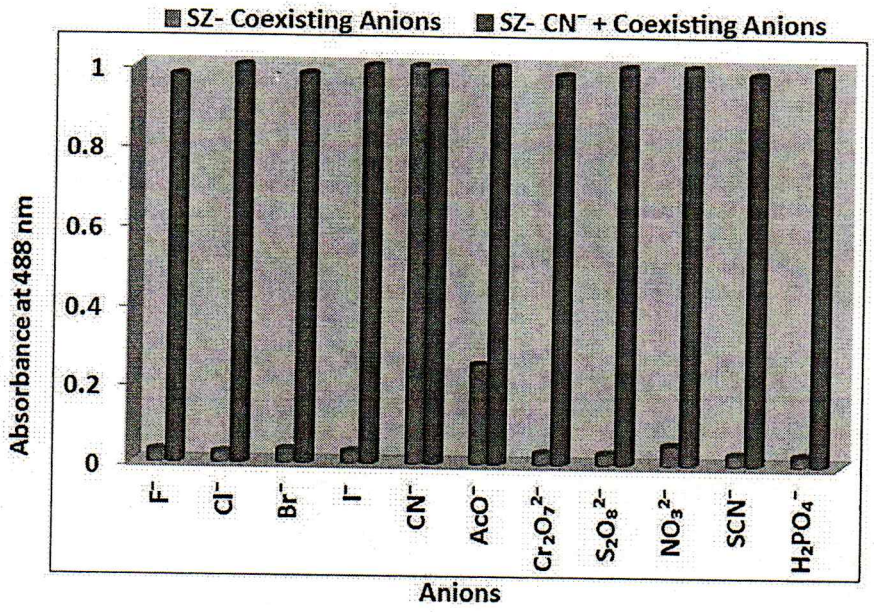

Fig. 2. UV–Vis absorbance responses of SZ in absence and presence of CN^- ion (150 μmol/L) and other competing anions (150 μmol/L) in MeCN: bis-tris buffer (9:1, v/v; pH = 7.0) solution at wavelength 488 nm.

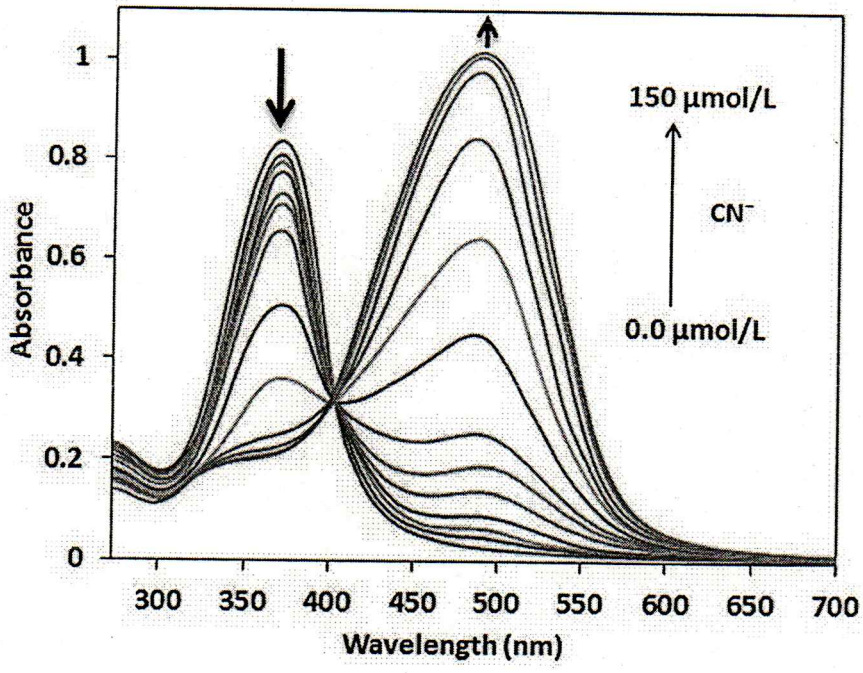

Fig. 3. UV–visible absorbance spectral changes of SZ (30 μmol/L) with increasing concentrations of CN^- in MeCN: bis-tris buffer (9:1, v/v; pH = 7.0) solution.

(TMS) as internal standard (δ in ppm). The elemental analyses were performed on a Vetro-ELIII elemental analyzer. ESI-Mass spectra were recorded on waters UPLC-TQD Mass spectrometer, UV–Vis absorption spectra were recorded on ELICO SL-210 UV–Vis double beam spectrophotometer at room temperature using a quartz cell with 1 cm path length, infrared (IR) spectra of sample and its complex were recorded on a Shimadzu FTIR-8400 spectrometer and pH values were measured by using digital pH-meter (Equip-Tronics EQ-614 A).

2.2. Synthesis of chemosensor

In a first step diazonium salt from *p*-nitroaniline was prepared according to the earlier reported method [34,35]. Similarly, in a second flask phenolate solution of vanillin was prepared by dissolving vanillin in NaOH and cooled to 0 °C and then a solution of diazonium salt was slowly added to the phenolate solution of vanillin placed in an ice bath with constant stirring for about one hour and then allowed to room temperature. The precipitate formed filtered and recrystallized in ethanol to give the desired dye (2-hydroxy-3-methoxy-5-[(*E*)-(4-nitrophenyl)diazenyl]benzaldehyde). Then the prepared dye (1 mmol) and *p*-toluidine (1 mmol) with little quantity of acetic acid were mixed in 40 mL of hot absolute ethanol and the resulting solution was refluxed for 9 h at 80 °C. The progress of the reaction was monitored by using TLC (*n*-hexane/ethyl acetate, 2:8, v/v), after completion of the reaction,

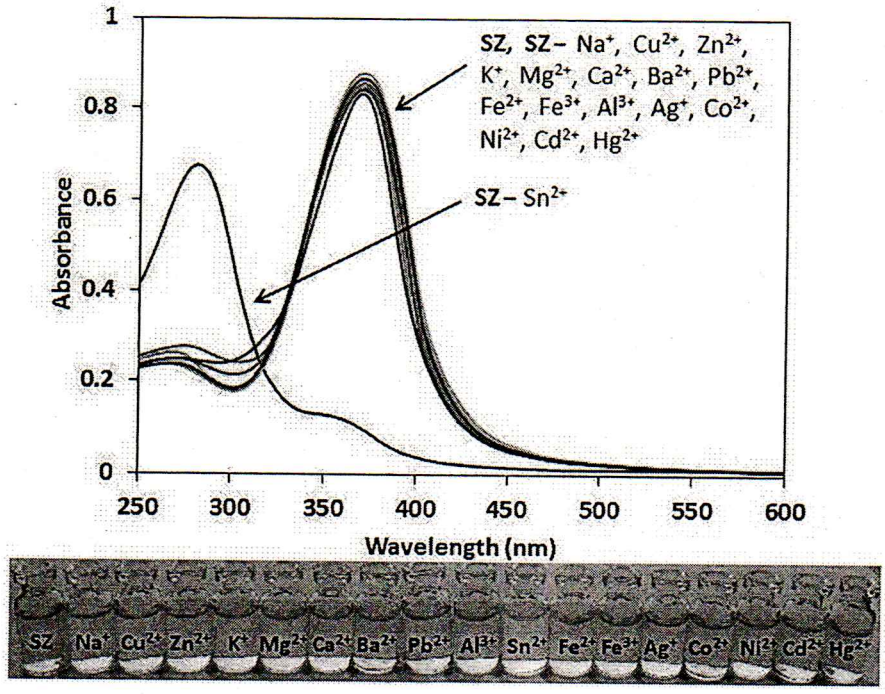

Fig. 4. UV–Vis absorbance spectra of **SZ** (30 μmol/L) in the presence of different cations (150 μmol/L) in MeCN: bis-tris buffer (9:1, v/v; pH = 7.0) solution.

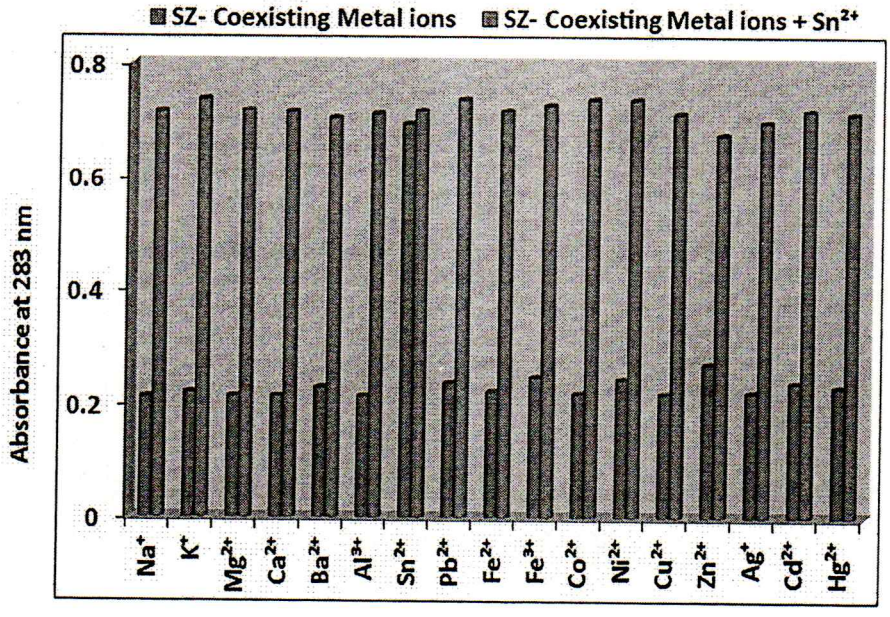

Fig. 5. Absorbance responses of **SZ** in absence and presence of Sn^{2+} ion (150 μmol/L) and several competing cations (150 μmol/L) in MeCN: bis-tris buffer (9:1, v/v; pH = 7.0) solution at wavelength 283 nm.

the reaction mixture cooled to room temperature and the precipitate obtained was filtered, washed with ethanol and recrystallized in DMF/H_2O to give reddish-brown solid (Scheme 1). (Yield, 74%), Melting point: > 300 °C; ^{1}H NMR (300 MHz, DMSO-d_6) δ (ppm), (Fig. S1): 2.36 (s, 3H, $-CH_3$), 3.73 (s, 3H, $-OCH_3$), 7.16–7.17 (d, 2H, HAr), 7.29–7.31 (d, 2H, HAr), 7.46–7.47 (s, 1H, HAr), 8.08–8.08 (s, 1H, HAr), 8.14–8.16 (d, 2H, HAr), 8.44–8.46 (d, 2H, HAr), 8.67 (s, 1H, CH), 10.58 (s, 1H, –OH); ^{13}C NMR (75 MHz, DMSO-d_6) δ (ppm), (Fig. S2): 20.9, 55.3, 99.9, 118.9, 122.8, 123.7, 123.9, 125.9, 131.4, 139.1, 146.9, 149.0, 150.3, 152.2, 157.3, 160.8; Anal. Calcd. for $C_{21}H_{18}N_4O_4$ (%): C 64.61, H 4.65, N 14.35. Found: C 64.76, H 4.68, N 14.57; MS (ESI-MS) *m/z* 391 $[SZ + H]^+$ (Fig. S3).

2.3. Experimental procedure

The stock solution of each cation and anion were prepared at 1.0×10^{-2} mol/L in MeCN: water and the stock solution of chemosensor 3×10^{-3} mol/L were prepared in acetonitrile. For UV–Visible absorbance spectral measurements sensor **SZ** was further diluted to 5 mL with MeCN: bis-tris buffer (9:1, v/v; pH = 7.0) to give desired concentration 30 μmol/L and then absorption spectra were recorded by adding 150 μmol/L of each ion to the solution of **SZ**.

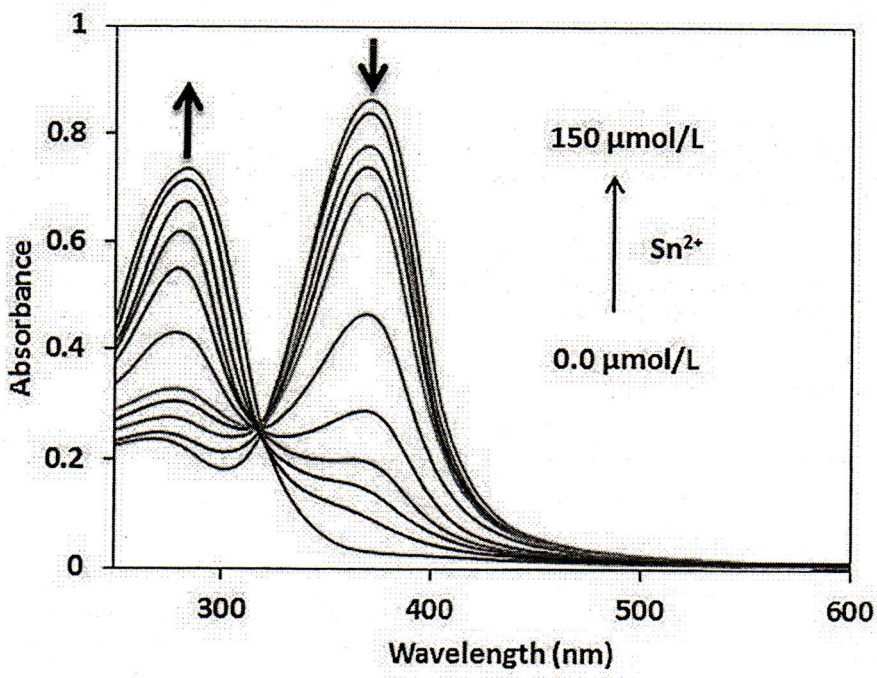

Fig. 6. UV–visible absorbance spectral changes of SZ (30 µmol/L) with increasing concentrations of Sn^{2+} in MeCN: bis-tris buffer (9:1, v/v; pH = 7.0) solution.

3. Result and discussion

3.1. Colorimetric sensing of anion

The chemosensing properties of chemosensor **SZ** (30 µmol/L) towards various anions such as F^-, Cl^-, Br^-, I^-, CN^-, AcO^-, $Cr_2O_7^{2-}$, $S_2O_8^{2-}$, NO_3^{2-}, SCN^-, $H_2PO_4^-$ in MeCN: bis-tris buffer (9:1, v/v; pH = 7.0) was investigated by visible color change and UV–Vis absorption spectral changes. As shown in Fig. 1, chemosensor **SZ** showed a high energy intramolecular charge transfer absorption band located at 371 nm attributed due to π-π* transition of azo and azomethine chromophores. Upon the addition of 150 µmol/L of each anion, **SZ** showed a distinct spectral change in the absorption spectrum in the presence of CN^- with a naked eye color change from yellow to pink. While other anions showed little or no absorption spectral changes of **SZ**. Indicating chemosensor **SZ** could be served as a naked eye colorimetric sensor for cyanide ion. This high selectivity of **SZ** to CN^- over other anions may be explained by the basicity (pKa) and hydrogen bonding of the anions in an aqueous medium. The basicity of the anions is supposed to be in order of $CN^- > AcO^- > F^- > H_2PO_4^- > Cl^- > HSO_4^- > SCN^- > NO_3^- > Br^- > I^-$ and that of hydrogen bonding ability based on electronegativity is as follows; $F^- > AcO^- > H_2PO_4^- > CN^-$, that is in aqueous medium the hydration energy of F^- ($\Delta H_{hyd} = -505$ kJ/mol) and AcO^- ($\Delta H_{hyd} = -375$ kJ/mol) are comparatively more than CN^- ($\Delta H_{hyd} = -67$ kJ/mol) [36]. Hence in aqueous medium CN^- has weak hydrogen bonding high basicity as compared to other anions such as F^-, AcO^- or SCN^- as a result, CN^- deprotonate phenolic proton of **SZ** and showing a new charge transfer band at 488 nm.

To further study the preferential selectivity of chemosensor **SZ** for CN^- competitive experiments was conducted in presence of various competing anions (F^-, Cl^-, Br^-, I^-, AcO^- $Cr_2O_7^{2-}$, $S_2O_8^{2-}$, NO_3^{2-}, SCN^-, $H_2PO_4^-$). For competitive experiment chemosensor **SZ** (30 µmol/L) was mixed with 150 µmol/L of CN^- and 150 µmol/L of other competitive anions. The results indicate that **SZ** shows good selectivity for CN^- in the presence of coexisting anions makes it useful in practical application for CN^- in the presence of coexisting anions (Fig. 2).

Based on the selectivity of the sensor **SZ** towards CN^-, the binding affinity of **SZ** (30 µmol/L) towards CN^- was further investigated by UV–visible titration experiment at different concentration levels of cyanide ion. Fig. 3 shows that with the gradual addition of CN^- from 0.0–150 µmol/L the absorption peak of **SZ** decreases gradually at 371 nm and a new absorption peak emerges at 488 nm with an isosbestic point at 403 nm indicating the formation of new intermediate in the reaction medium. Furthermore, a large red shift of 117 nm in absorption spectra of **SZ** led us to the transition of internal charge transfer (ICT) band through the deprotonation phenolic −OH proton attached with electron-deficient $-NO_2$ group by the CN^- ion, is mainly due to the π delocalization of aromatic proton which reduces the energy gap of p-p transition [37] results a new absorption band at 488 nm with remarkable color change from yellow to pink.

Also, the stoichiometry of chemosensor **SZ** and CN^- ion complex was determined by Job's plot method [38] by considering the sum of the concentration of CN^- and **SZ** constant and varying the mole fraction from 0.1 to 0.9. The Job's plot reached a maximum value at 0.5 confirming that, 1:1 stoichiometry complex between **SZ** and CN^- (Fig. S4) with binding constant; Ka = $1.702 \times 10^3\ M^{-1}$ determined by using the Benesi-Hildebrand Eq. (1) [39] (Fig. S5),

$$\frac{1}{A\text{-}A_0} = \frac{1}{Ka(A_{max} - A_0)[CN^-]} + \frac{1}{A_{max} - A_0} \quad (1)$$

Moreover, to validate the chemosensing performance of **SZ** in a real sample, the experimental data obtained from UV–Vis titration for a concentration of CN^- were plotted to obtain a linear relationship. Fig. S6 showed **SZ** gives a good linear relationship in the calibration graph ($A–A_0$) as a function of CN^- concentrations at wavelength 488 nm in the range 1.5–75 µmol/L with correlation coefficient 0.9972. Moreover, after the gradual addition of 75 µmol/L of CN^-, no further variation is observed in the absorption spectra of **SZ** indicating that the **SZ** reached a saturable concentration of CN^- (Fig. S7). Importantly, the plot of ($A–A_0$) against the concentration of CN^- fit a linear Beer-Lambert equation.

The limit of detection (LOD) was calculated by Eq. (2) [40],

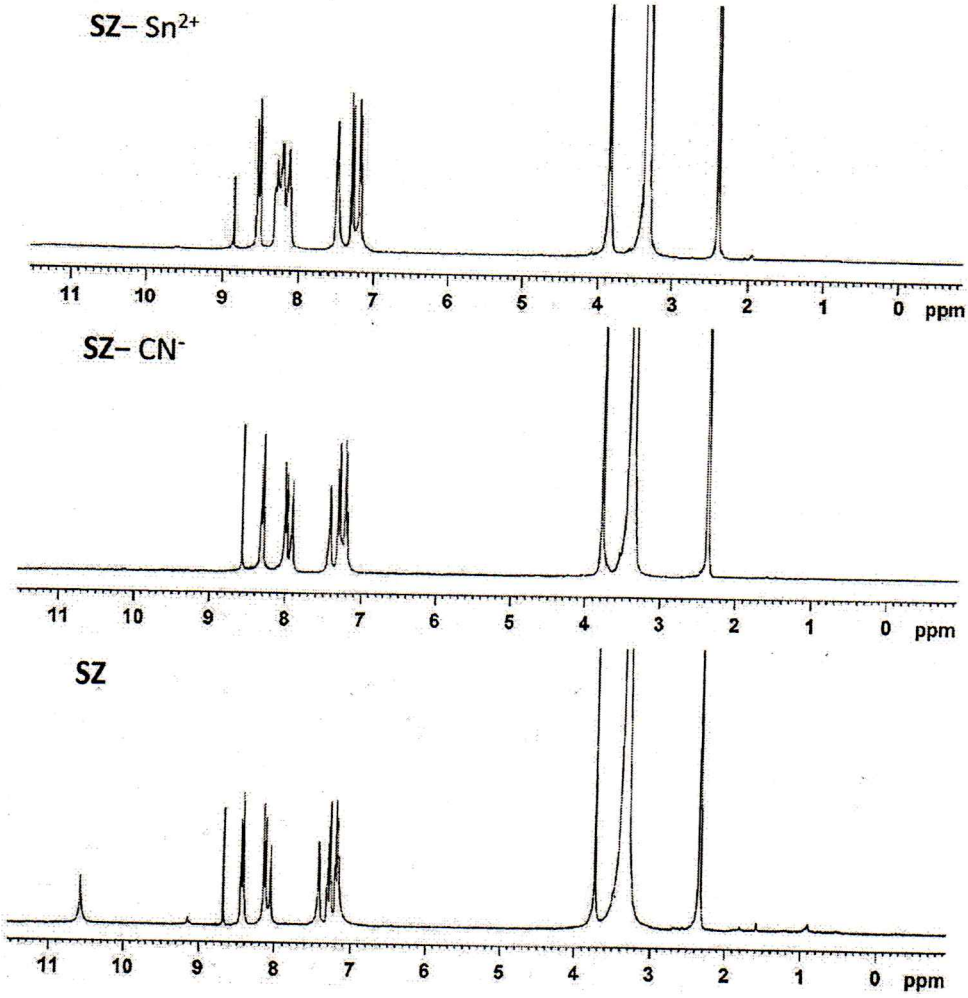

Fig. 7. ^{1}H NMR spectra of SZ in absence and presence of CN^{-} and Sn^{2+} ion.

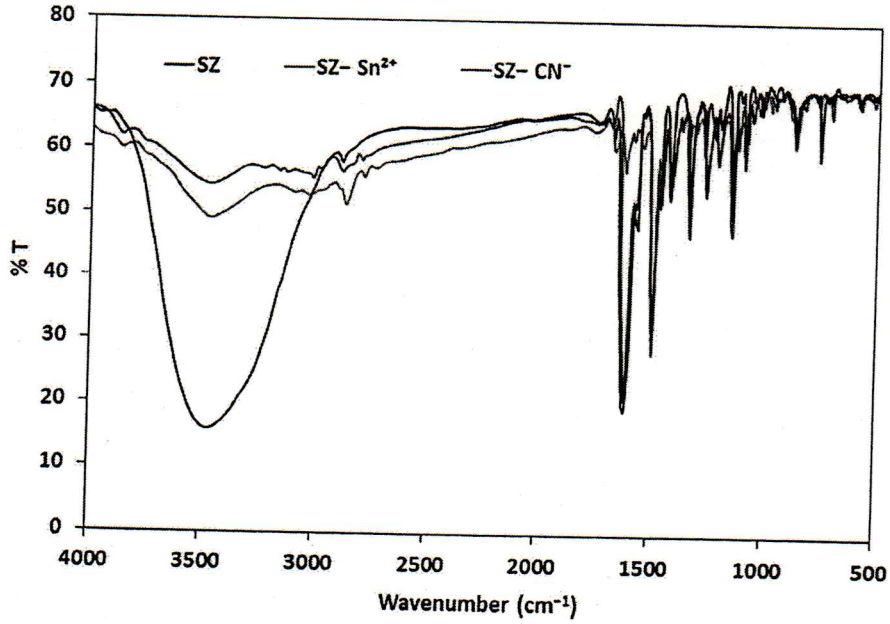

Fig. 8. IR spectra of chemosensor SZ, SZ– CN^{-} and SZ– Sn^{2+}.

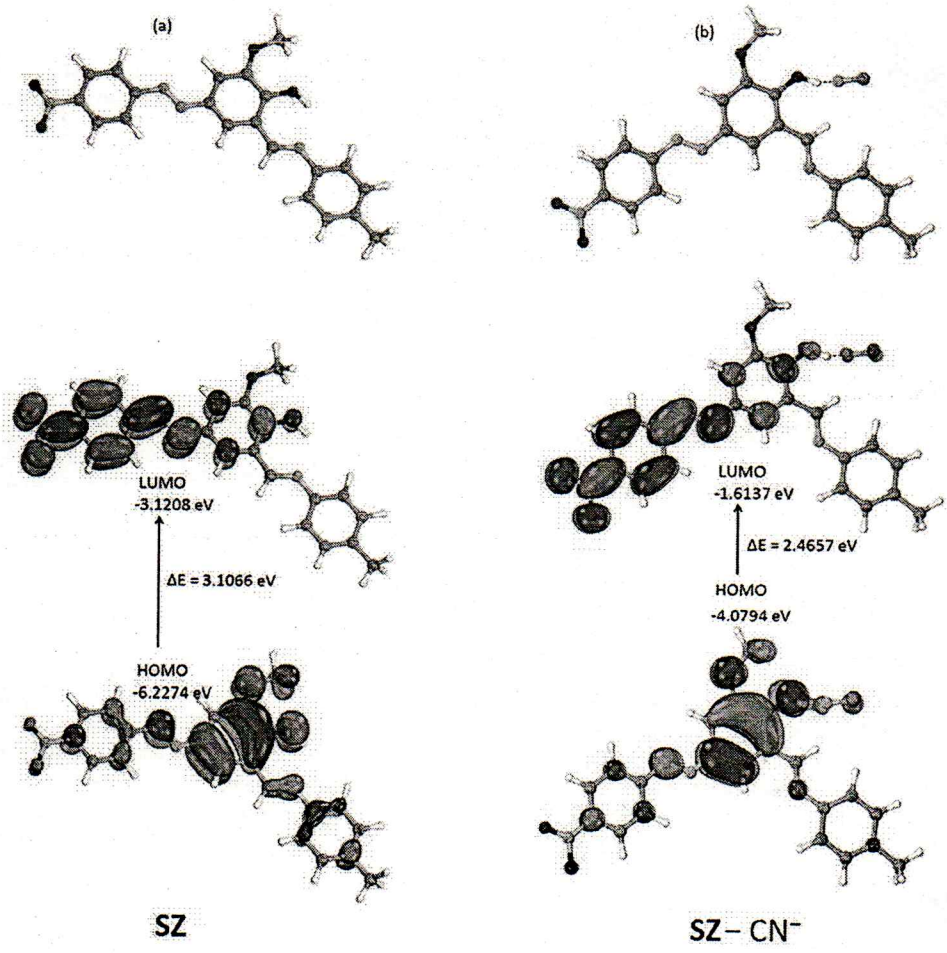

Fig. 9. Geometry optimized structure and HOMO and LUMO energy level of (a) **SZ** and (b) **SZ**– CN^-.

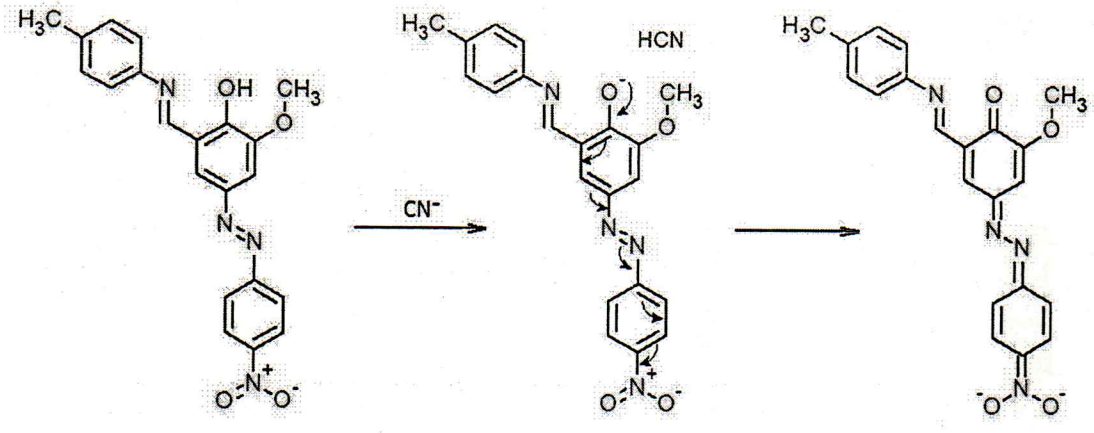

Scheme 2. Proposed binding mode of chemosensor **SZ** for CN^-.

$$LOD = \frac{3\sigma}{k} \quad (2)$$

where σ is the standard deviation of the y-intercept of the regression line and k is the slope of the calibration curve. Here, the colorimetric LOD for CN^- is 0.649 μmol/L which is lower than the maximum permitted level of cyanide in drinking water regulated by world health organization (1.9 μmol/L) [41].

3.2. Colorimetric sensing of cation

The colorimetric sensing study of chemosensor **SZ** was further carried towards biologically important cations including (Na^+, K^+, Mg^{2+}, Ca^{2+}, Ba^{2+}, Al^{3+}, Sn^{2+}, Pb^{2+}, Fe^{2+}, Fe^{3+}, Co^{2+}, Ni^{2+}, Cu^{2+}, Ag^+, Zn^{2+}, Cd^{2+}, Hg^{2+}) by naked eye and UV–Visible absorption spectra measurements in MeCN: bis-tris buffer (9:1, v/v; pH = 7.0). Fig. 4 shows upon the addition of 150 μmol/L of each cation, only Sn^{2+} shows a significant increase in the intensity of the absorption spectrum at

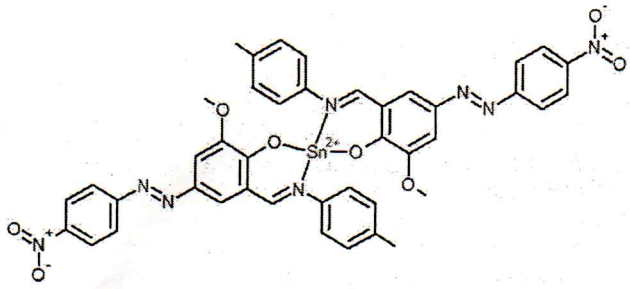

Scheme 3. Proposed binding mode of chemosensor **SZ** for Sn^{2+}.

283 nm and color changes from yellow to colorless with a hypsochromic shift. At the same experimental conditions, other cations did not induce any spectral or color change of the **SZ**. Thus, sensor **SZ** can be used for the colorimetric detection of Sn^{2+} in an organic-aqueous medium.

To further study the selectivity of **SZ** as a colorimetric chemosensor for Sn^{2+}, competition experiments were conducted in the presence of other competitive cations. For a competitive experiment, 30 μmol/L of sensor **SZ** was treated with 150 μmol/L of Sn^{2+} in presence of other competitive cations (150 μmol/L). As shown in Fig. 5 no interference was observed for the detection of Sn^{2+} in the presence of competitive cations. Hence, **SZ** shows better selectivity over other tested competitive cations with a notable color change from yellow to colorless.

Moreover, the UV–Vis titration experiment with different concentrations of Sn^{2+} ion was conducted by using 30 μmol/L solution of **SZ** to examine the binding affinity of **SZ** with Sn^{2+}. Fig. 6 shows the gradual addition of Sn^{2+} from 0.0 to 150 μmol/L. to the solution of **SZ**, absorption band emerges at 283 nm with an isosbestic point at 318 nm signifying conversion of **SZ** into a single **SZ**– Sn^{2+} species which may be due to the LMCT and the selectivity of **SZ** to Sn^{2+} is according to the Pearson's hard-soft acid-base theory [42], nitrogen from imine (HC=N) is a middle-intensity base and Sn^{2+} is a soft borderline acid. Therefore, Sn^{2+} is likely to form its stable complex with **SZ**.

To get a clear understanding of the stoichiometry of the **SZ**– Sn^{2+} complex, Job's plot method was conducted [38]. The Job's plot analysis shows a maximum of 0.33 representing 2:1 stoichiometry between **SZ** and Sn^{2+} ion (Fig. S8). Besides, from the UV–Vis titration experimental data for the concentration of Sn^{2+}, the binding constant of **SZ** for Sn^{2+} was estimated to be; Ka = 4.195×10^3 M^{-1} using equation (3) (Fig. S9) [39],

$$\frac{1}{A\text{-}A_0} = \frac{1}{Ka(A_{max} - A_0)[Sn^{2+}]} + \frac{1}{A_{max} - A_0} \quad (3)$$

Furthermore, the LOD for Sn^{2+} was measured by using the formula 3σ/k is found to be 0.754 μmol/L with correlation coefficient 0.9959.

3.3. Effect of pH

For successful practical application of chemosensor **SZ**, proper pH condition of the sample solution is an important factor that affects the spectral properties of the **SZ**. The effect of pH on the absorption spectrum of the **SZ** was studied in the pH range 2–12 by using bis-tris buffer solution and the pH value of buffer solution was adjusted by mixing a diluted solution of HCl and NaOH. The results of changes in the absorption intensity of the **SZ** at 488 nm and 283 nm were recorded in the presence of CN^- and Sn^{2+} ion as shown in Fig. S12. In the presence of CN^- and Sn^{2+}, **SZ** shows maximum and stable absorbance intensity in the pH range 6–10. Therefore, the present work was carried at pH = 7.0 by using the bis-tris buffer at room temperature.

3.4. NMR, IR and ESI-MS studies for CN^- and Sn^{2+}

To explore the sensing mechanism of chemosensor **SZ** towards CN^- and Sn^{2+}, ^1H NMR titration experiment, IR and ESI-MS studies were performed. Fig. 7 shows the ^1H NMR spectra of sensor **SZ** in the absence and presence of CN^- and Sn^{2+} in DMSO-d_6. In the absence of CN^- and Sn^{2+}, **SZ** shows singlet resonance peak at δ = 10.58 and 8.67 ppm for phenolic proton and imine proton respectively. When 30 μmol/L of CN^- was added to the sensor **SZ**, the phenolic proton peak at δ = 10.58 (s, 1H) ppm almost disappeared, and other aromatic ring protons specifically phenyl protons possessing –OH group are involved in delocalization show small upfield shifts. Indicates that deprotonation of phenolic –OH group of **SZ** by CN^- may be delocalized through the whole molecule during the recognition process. Similarly, upon the addition of 15 μmol/L of Sn^{2+} to sensor **SZ**, the phenolic –OH proton peak at δ = 10.58 (s, 1H) ppm completely disappeared and the imine proton peak at δ = 8.67 (s, 1H) ppm shifted downfield to δ = 8.85 ppm along with marginal downfield of aromatic proton peaks. Indicating the phenolic –OH and nitrogen (–CH=N–) of **SZ** takes part in the complexation.

Furthermore, Fig. 8 shows the IR spectrum of the **SZ** in the absence and presence of CN^- and Sn^{2+}. In the IR spectrum of the **SZ**, the stretching absorption peaks of HC=N appeared at 1624 cm^{-1} and a broad as well as in-plane bending vibration peak of –OH observed around at 3400 cm^{-1} and 1320 cm^{-1} respectively. After the interaction

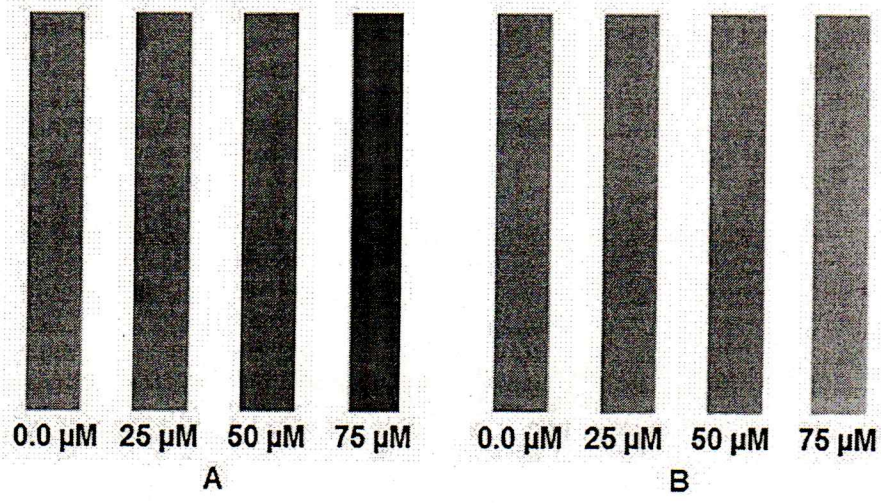

Fig. 10. Photographs of the filter paper coated with **SZ** in different concentrations of **(A)** CN^- and **(B)** Sn^{2+}.

Table 1
Determination of CN^- in industrial wastewater samples via a standard addition method (n = 3).

Name of the sample	Amount of Standard CN^- Added (μmol/L)	Total CN^- found (n = 3) (μmol/L)	Recovery of CN^- added (n = 3) (%)	RSD (%)	Relative Error (%)
Industrial waste-water I	20.0	20.27	101.39	0.85	1.39
	30.0	30.32	101.06	0.85	1.06
Industrial waste-water II	20.0	20.36	101.81	0.71	1.81
	30.0	30.77	102.57	0.61	2.57

Industrial estate, Ichalkaranji (West Maharashtra, India)

with CN^-, the vibrational peak corresponds to the –OH proton get reduced while this spectrum shows the stretching absorption peaks of the HC=N group. However, upon complexation with Sn^{2+}, the absorption vibration peaks of HC=N and –OH almost disappeared. Indicates that, CN^- deprotonate the phenolic –OH group and Sn^{2+} had complexation with imine (HC=N) nitrogen and phenolic –OH group of **SZ**. To get further information for the binding mode of the **SZ**– Sn^{2+} complex, ESI-MS study was carried out. As shown in Fig. S13, the positive ion the peak at *m/z* 899 was corresponding to $[2SZ + Sn^{2+} - 1H]^+$, which provides strong evidence for the 2:1 stoichiometry between **SZ** and Sn^{2+}.

3.5. DFT studies

In addition, to better understand the binding mode of sensor **SZ** with CN^- ions, theoretical studies were performed by using the ORCA program package (version 3.0.3). The geometries of **SZ** and **SZ**– CN^- complex were optimized by using B3LYP/def2-TZVP [43,44]. As shown in Fig. 9, the electron density of **SZ** at HOMO is mainly spread over the entire molecule whereas unoccupied orbital LUMO is localized mainly on 4-[(*E*)-(4-nitrophenyl)diazenyl]phenol unit. On complexation of the **SZ** with CN^-, HOMO is localized on 4-diazenyl-2-methoxyphenol moiety and LUMO is localized on 2-methoxy-4-[(E)-(4-nitrophenyl) diazenyl]phenol moiety. Likewise, the energy band gap (ΔE) between HOMO and LUMO of **SZ** and corresponding **SZ**– CN^- were decreased from 3.1066 eV to 2.4657 eV respectively. These results predicted intramolecular charge transfer from 4-diazenyl-2-methoxyphenol to 2-methoxy-4-[(E)-(4-nitrophenyl)diazenyl] phenol moiety induced by CN^- ion and is in closed agreement with the new charge transfer absorption band observed at 488 nm in the UV–Visible spectra.

Thus by considering the above results, the sensing mechanism of chemosensor **SZ** for CN^- and Sn^{2+} was shown in Scheme 2 and Scheme

3.6. Applications of the proposed chemosensor SZ

3.6.1. Solid-state detection of CN^- and Sn^{2+}

To explore the practical application of **SZ** for quantitative, quantitative and on-site detection of CN^- and Sn^{2+} ion the test strips of chemosensor **SZ** were prepared by immersing Whatman filter paper into solution of chemosensor (1 mmol) prepared in MeCN: bis-tris buffer (9:1, v/v, pH = 7.0), dried in air and then the test strips were dipped in aqueous solution of CN^- and Sn^{2+} prepared at different concentration. An immediate color change was observed from yellow to pink and yellow to colorless respectively. As depicted in Fig. 10 the expected LOD of test strip coated with **SZ** for CN^- and Sn^{2+} was 25 μmol/L.

3.6.2. Determination of CN^- from industrial waste water

To check practical utility, the proposed chemosensor **SZ** was successfully applied for the determination of CN^- in industrial waste water samples collected from Industrial estate, Ichalkaranji (West Maharashtra, India). The collected water samples were first filtered through Whatman No. 41 filter paper to remove suspended solid material, impurities, etc. After that, samples were spiked with a standard solution of CN^- ions at two different concentration levels and finally diluted within the working linear range and examined with the proposed method by standard addition method [40,45]. The results are summarized in Table 1 which shows that the chemosensor **SZ** can measure the concentration of CN^- in water samples with good recoveries in the range of 101.23% and 102.19%. Hence, the chemosensor **SZ** can be applicable for CN^- determinations in different water samples.

4. Conclusions

In conclusion, we have developed a simple and cost-effective azo linked Schiff base as a colorimetric chemosensor (**SZ**) for selective detection of CN^- and Sn^{2+} over other competitive ions in CH_3CN: bis-tris buffer (9:1, v/v) medium. **SZ** displayed remarkable changes in absorption band and significant color change in the presence of CN^- and Sn^{2+} with detection limit 0.649 μmol/L and 0.754 μmol/L respectively. Binding mechanism of **SZ** for CN^- and Sn^{2+} was studied by ^1H NMR, IR and ESI-MS studies. Furthermore, DFT studies were supported the experimental result and sensing mechanism for CN^- is due to ICT. Importantly, chemosensor **SZ** was also successfully applied for quantitative detection of CN^- in an industrial wastewater sample and colorimetric test kit was designed for quantitative and onsite detection of CN^- and Sn^{2+}.

Acknowledgments

Authors are thankful to Shivraj College, Gadhinglaj, Department of Chemistry; Shivaji University, Kolhapur and SAIF CSIR-CDRI, Lucknow, India for providing the all necessary infrastructural and instrumental facility. One of the author AHG gratefully acknowledges DST-SERB, New Delhi for providing research grants under young scientist scheme (File no. YSS/2015/001806).

Appendix A. Supplementary data

Supplementary data to this article can be found online at https://doi.org/10.1016/j.ica.2019.119372.

References

[1] J.F. Zhang, Y. Zhou, J. Yoon, J.S. Kim, Chem. Soc. Rev. 40 (2011) 3416–3429.
[2] D. Yun, J.B. Chae, C. Kim, J. Chem. Sci. 131 (2019) 10.
[3] J.L. Atwood, J.E. Davies, D.D. MacNicol, F. Vogtle, Comprehensive Supramolecular Chemistry, Pergamon Press, New York, NY, 1996.
[4] B. Valeur, I. Leray, Coord. Chem. Rev. 205 (2000) 3–40.
[5] P.D. Beer, P.A. Gale, Angew. Chem. Int. Ed. Engl. 40 (2001) 486–516.
[6] L.E. Santos-Figueroa, M.E. Moragues, E. Climent, A. Agostini, R. Martinez-Manez, F. Sancenon, Chem. Soc. Rev. 42 (2013) 3489–3613.
[7] W.J. Qu, W.T. Li, H.L. Zhang, T.B. Wei, Q. Lin, H. Yao, Y.M. Zhang, Sensors Actuators B 241 (2017) 430–437.
[8] B. Vennesland, E.E. Comm, C.J. Knowles, J. Westly, F. Wissing, Cyanide in Biology, Academic Press, London, 1981.
[9] A. Alizadeh, S. Ghouzivand, M.M. Khodaei, M. Ardalani, J. Chem. Sci. 128 (2016) 537.
[10] N. Kuyucak, A. Akcil, Miner. Eng. 50–51 (2013) 13–29.
[11] D.W. Boening, C.M. Chew, Water Air Soil Pollution 109 (1999) 67–79.
[12] Y. Feng, L. Bai, S. Wang, X. Kong, L. Cong, Q. Zhao, Q. Yang, Y. Li, Chem. Res. Chin. Univ. 33 (2017) 534–539.
[13] R.R. Dash, A. Gaur, C. Balomajumder, J. Hazard. Mater. 163 (2009) 1–11.

[14] H.J. Keene, L.L. Shklair, G.J. Mickel, M.R. Wirthlin, J. Dent. Res. 56 (1977) 5–10.
[15] C.S. Cho, H.K. Lim, S.C. Shim, T.J. Kim, H.J. Choi, Chem. Commun. 3 (1998) 995–996.
[16] K.K. Upadhyay, R.K. Mishra, A. Kumar, Catal. Lett. 121 (2008) 118–120.
[17] A.B. Ferreira, A.L. Cardoso, M.J. da Silva, ISRN Renewable Energy 2012 (2012) 13.
[18] M. Nath, Appl. Organomet. Chem. 22 (2008) 598–612.
[19] H. Rudel, Ecotoxicol. Environ. Saf. 56 (2003) 180–189.
[20] **J.M. Gardlik, D.S. Stevens, B.G. Comstock, Methods of regulating hair growth using metal complexes of oxidized carbohydrates, US Patent App. 09/909, 441, 2002.**
[21] C. Byrne, S.D. Divekar, G.B. Storchan, D.A. Parodi, M.B. Martin, J. Mammary Gland Biol. Neoplasia 18 (2013) 63–73.
[22] N. Cardarelli, Thymus 15 (1990) 223–231.
[23] L.R. Sherman, J. Masters, R. Peterson, S. Levine, J. Anal. Toxicol. 10 (1986) 6–9.
[24] T.T. Christison, J.S. Rohrer, J. Chromatogr. A 1155 (2007) 31–39.
[25] A. Safavi, N. Maleki, H.R. Shahbaazi, Anal. Chim. Acta 503 (2004) 213–221.
[26] K. Boutakhrit, Z.P. Yang, J.M. Kauffmann, Talanta (1995) 1883–1890.
[27] D.G. Themelis, S.C. Karastogiann, P.D. Tzanavaras, Anal. Chim. Acta 632 (2009) 93–100.
[28] R.W. Dabeka, A.D. McKenzie, R.H. Albert, J. Assoc. Off. Anal. Chem. 68 (1985) 209–213.
[29] E.J. Cho, B.J. Ryu, Y.J. Lee, K.C. Nam, Org. Lett. 7 (2005) 2607–2609.
[30] A. Mohammadi, S. Yaghoubi, Sens. Actuators B 241 (2017) 1069–1075.
[31] A.L. Berhanu, Gaurav, I. Mohiuddin, A.K. Malik, J.S. Aulakh, V. Kumar, K.H. Kim, Trends Anal. Chem. 11 (2019) 74–91.
[32] P. Zhang, B.B. Shi, T.B. Wei, Y.M. Zhang, Q. Lin, H. Yao, X.M. You, Dyes Pigm. 99 (2013) 857–862.
[33] M. Orojloo, S. Amani, Talanta 159 (2016) 292–299.
[34] A. Mohammadi, M.R. Yazdanbakhsh, L. Farahnak, Spectrochim. Acta A 89 (2012) 238–242.
[35] M.R. Yazdanbakhsh, A. Mohammadi, J. Mol. Liq. 148 (2009) 35–39.
[36] J.J. Lee, G.J. Park, Y.W. Choi, G.R. You, Y.S. Kim, S.Y. Lee, C. Kim, Sens. Actuators, B 207 (2015) 123–132.
[37] N. Maurya, S. Bhardwaj, A.K. Singh, Sens. Actuators B 229 (2017) 483–491.
[38] W. Likussar, D.F. Boltz, Anal. Chem. 43 (1971) 1273–1277.
[39] H. Benesi, J. Hilderbrand, J. Am. Chem. Soc. 71 (1949) 2703–2707.
[40] **ICH, ICH Harmonised Tripartite Guideline: Validation of Analytical Procedures: Text and Methodology, Q2 (R1), ICH, Geneva, Switzerland, 2005. Available at** http://www.ich.org/fileadmin/Public_Web_Site/ICH_Products/Guidelines/Quality/Q2_R1/Step4/Q2_R1 Guideline.pdf.
[41] **World Health Organization, Guidelines for Drinking-Water Quality, third ed., World Health Organization, Geneva, 2008, p. 188.**
[42] R.G. Pearson, J. Am. Chem. Soc. 85 (1963) 3533–3539.
[43] A. Schaefer, H. Horn, R. Ahlrichs, J. Chem. Phys. 97 (1992) 2571–2577.
[44] F. Weigend, R. Ahlrichs, PCCP 7 (2005) 3297–3305.
[45] V.D. Suryawanshi, A.H. Gore, P.R. Dongare, P.V. Anbhule, S.R. Patil, G.B. Kolekar, Spectrochim. Acta A 114 (2013) 681–686.